energy&fuels

Article

Cite This: Energy Fuels 2018, 32, 2901−2907

pubs.acs.org/EF

Positive Ion Electrospray Ionization Suppression in Petroleum and Complex Mixtures

Brian M. Ruddy,[†] Christopher L. Hendrickson,[*,†,‡] Ryan P. Rodgers,[*,†,‡] and Alan G. Marshall[*,†,‡]

[†]Department of Chemistry and Biochemistry, Florida State University, Tallahassee, Florida 32306 United States

[‡]National High Magnetic Field Laboratory, Florida State University, 1800 East Paul Dirac Drive, Tallahassee, Florida 32310-4005 United States

Supporting Information

ABSTRACT: Since the emergence of high resolving power crude oil mass spectrometry two decades ago, hundreds of publications and presentations have detailed petroleum complex mixtures by electrospray ionization (ESI) mass spectrometry (MS). None of these works have reported or detailed ion suppression (also referred to as ionization biasing or matrix effects) which is a well-known feature of ESI. Here, we show the extreme consequences of ionization biasing within a narrow, 1 order of magnitude concentration range for crude oil mixture direct infusion experiments in positive ion (+) ESI. An oil spill contaminant, a crude oil, and an equimolar model compound mixture were electrosprayed at various analyte and acid modifier concentrations for Fourier transform ion cyclotron resonance (FT-ICR) and time-of-flight (TOF) MS analysis. A 3-fold increase in the number of elemental compositions is achieved by optimization of analyte and acid concentration. At high analyte concentration, oxygen heteroatom class (i.e., $C_cH_hO_x$ species, denoted henceforth simply as O_x) abundance is attenuated and practically nullified. The suppression can be understood from (+) ESI TOF mass analysis of a prepared equimolar model compound mixture, particularly those with ketone functional groups. At sufficiently low concentration of analyte, the relative abundances of nitrogen- and oxygen-containing model compounds no longer vary. For (+) ESI at the flow rates and voltages described in this study, we recommend operating at mass/volume petroleum residue concentration below 0.1 mg/mL in 1:1 (v:v) toluene/methanol with formic acid at 2.5% (v:v).

INTRODUCTION

Dating from the application of ultrahigh resolution mass spectrometry to the characterization of petroleum crude oils,[1−4] there has been great interest in ionization techniques that access a wide range of molecular elemental compositions: electrospray ionization,[5,6] laser desorption/ionization,[7] field desorption/ionization,[8] supersonic molecular beam/electron ionization,[9] atmospheric pressure chemical ionization,[10] atmospheric pressure photoionization,[11] sonic spray ionization,[12] desorption electrospray ionization,[13,14] laser-induced acoustic desorption,[15,16] infrared/ultraviolet two-laser desorption/ionization,[17] direct analysis in real time,[18,19] and laserspray ionization.[20] Electrospray ionization[21,22] was first introduced to petroleum analysis by Zahn and Fenn[5] and preferentially ionizes the most polar compounds in complex organic mixtures. Positive ion electrospray ionization typically relies on protonation of basic compounds by an acid (e.g., formic acid, acetic acid, or trifluoroacetic acid) to form quasimolecular even-electron $[M + H]^+$ cations. Similarly, negative ion electrospray relies on a suitable base (e.g., ammonium hydroxide, tetramethylammonium hydroxide)[23] to deprotonate acids to form quasimolecular even-electron $[M - H]^-$ anions. Thus, the most efficiently ionized electrosprayed components of crude oil are typically 6-membered ring pyridinic nitrogen (positive ions)[24] and carboxylic acids (negative ions).[25,26]

Electrospray ionization suppression[27−29] (also reported as matrix effects,[30−34] ionization bias,[35] or hydrophobic bias[36]) has been well studied.[37−39] The phenomenon is important to quantitative method development,[34] for which relative ion numbers and robustness of detection is paramount. Thus, many studies combatting suppression have featured front-end liquid chromatography.[28−30,34] Sample cleanup,[32] spray solutions/modifiers,[29,30,36] inlet capillary length,[35] temperature,[3,9] and flow rate[32] have all been targets to reduce suppression.

Ionization suppression is believed to be caused by surface charge competition during droplet formation and therefore exacerbated by increased analyte concentration relative to solution charge.[31,33] At low analyte concentration and lower matrix complexity[30,32,34] response curves become linear,[31] consistent with the present results (see below). Here, we demonstrate ionization suppression in direct infusion crude oil mass spectrometry and the strong dependence of electrosprayed positive ion relative abundances on concentration. FT-ICR mass spectra of complex mixtures (an oil spill contaminant and a crude oil containing five times less oxygen based on bulk elemental analysis) were performed to observe the preferences. The results are then modeled from TOF mass analysis of an equimolar mixture of six simple N_1 and O_1 heteroatom class representative model compounds.

EXPERIMENTAL METHODS

FT-ICR Experiments and Samples. An oil spill contaminant from Pensacola Beach, Florida and a crude oil from the Gulf of Mexico provided complex mixtures for FT-ICR MS. The Soxhlet-extracted oil spill contaminant sample was reconstituted in toluene to yield a stock solution of 5 mg/mL. The stock solutions were further diluted to 1.0, 0.5, and 0.1 mg/mL in 1:1 (v:v) toluene/methanol and 2.5% (v:v)

Received: October 18, 2017
Revised: January 22, 2018
Published: February 16, 2018

ACS Publications © 2018 American Chemical Society

DOI: 10.1021/acs.energyfuels.7b03204
Energy Fuels 2018, 32, 2901−2907

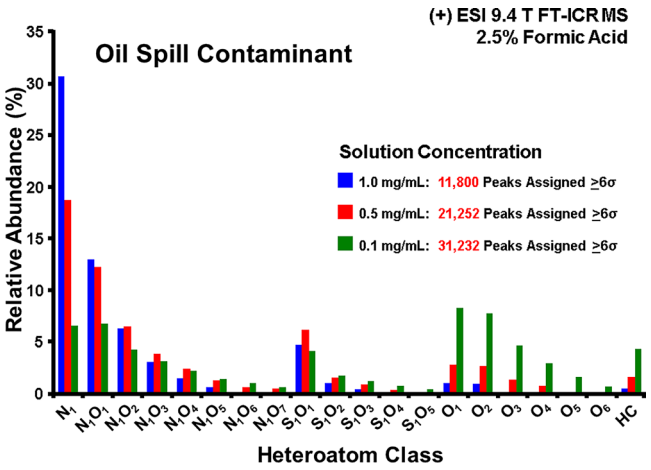

Figure 1. Heteroatom class distribution for (+) ESI oil spill contaminant at 2.5% percent formic acid concentration and analyte concentration 1.0 (blue), 0.5 (red), and 0.1 mg/mL (green). Note the much wider compositional coverage at lower analyte/formic acid ratio.

formic acid. The crude oil was also reconstituted in toluene to yield a stock solution of 5.0 mg/mL and diluted to 0.5, 0.25, 0.10, and 0.05 mg/mL in 1:1 (v:v) toluene/methanol and 2.5% (v:v) formic acid. Acid solutions were prepared at 10.0, 5.0, 2.0, 1.0, and 0.0% (v:v) in methanol and then diluted 1:1 (v:v) with 0.2 mg of oil spill contaminant in toluene mixture to make 5.0, 2.5, 1.0, 0.5, and 0.0% (v:v) final acid concentration and 0.1 mg/mL oil spill contaminant concentration. All FT-ICR experiments were performed with a custom-built mass spectrometer equipped with a passively shielded 9.4 T superconducting horizontal solenoid magnet (Oxford Instruments).[40] Samples were pumped through a fused silica capillary at 0.5 μL/min through a 50 μm i.d. fused silica microESI needle under typical ESI conditions (needle, 2.3 kV; tube lens, 350 V; heated metal capillary current, ~5.0 A). Time-domain data were acquired and processed by a Predator data station,[41] as described elsewhere.[42]

Because of the very high compositional complexity of the oil spill contaminant (more than twice as many peaks as the crude oil, including several thousand 1.7 mDa splits), broadband phase correction[43] was applied to all mass spectra to increase mass resolving power by up to a factor of 2.[44−47] Peak lists for the samples were generated, organized, and calibrated by use of custom modular software[41] equipped with walking calibration.[48] Multiplication of IUPAC mass by 14/14.01565 effectively converts the mass of CH_2 from 14.01565 to exactly 14.00000 to yield homologous Kendrick mass[49] series that contain the same double bond equivalents (DBE = number of heteroatoms and rings plus double bonds) but differ only by the number of CH_2 groups, to facilitate calibration and assignment of abundant series that span the entire mass range.

Time-of-Flight Mass Spectra of Model Compounds. An equimolar model compound mixture (30 mM each of 1-naphthol, dibenzofuran, 4,4′-dimethylbenzophenone, 7,9 dimethylbenzacridine, 2-aminoanthracene, and 2,6-dimethylquinoline) obtained from Sigma-Aldrich (St. Louis, MO)) was prepared in 1:1 (v:v) toluene/methanol. The mixture was serially diluted to 10, 1, 10^{-1}, 10^{-2}, 10^{-3}, 10^{-4}, 10^{-5}, 10^{-6}, and 10^{-7} mM in 1:1 (v:v) toluene/methanol and 2.5% (v:v) formic acid, and each solution was electrosprayed into a TOF mass spectrometer (Waters Micromass LCT Premier XE (Manchester, U.K.)) at 20 μL/min for positive ion analysis. All solvents were HPLC grade or better (J.T. Baker, Phillipsburg, NJ).

RESULTS AND DISCUSSION

Complex Mixture Analysis. Figure 1 displays the positive ion electrospray FT-ICR MS heteroatom class distribution for an oil spill contaminant at three concentrations. Here, reduction of analyte concentration from 1.0 to 0.1 mg/mL at constant ion accumulation period and acid concentration (2.5% by volume) results in increased relative abundance of oxygen classes and a nearly tripled number of assigned peaks. Figure 2 shows mass spectral segments (m/z 542−547) for the samples of Figure 1. At high analyte concentration (1.0 mg/mL, top), ions of the N_1 heteroatom class dominate the mass spectrum and appear at even nominal mass (in accordance with the nitrogen rule for even-electron ions[50]). Reduction in analyte concentration to 0.5 mg/mL (middle) and further to 0.1 mg/mL (bottom) results in increased number and relative abundance of oxygen-containing (O_x) ions at odd nominal mass, eventually exceeding N_1 class relative abundance at the lowest analyte concentration. Ultrahigh mass resolving power (622 000 average at m/z 500) enables generation of the heteroatom class

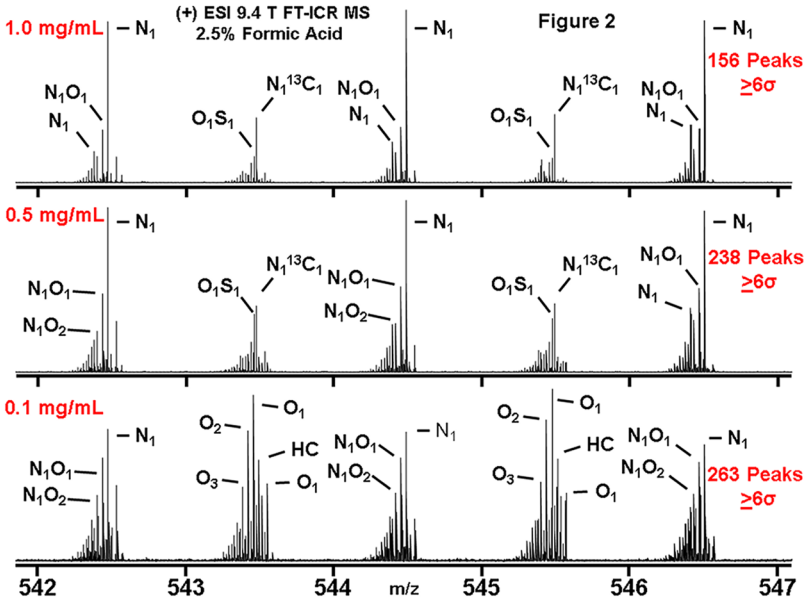

Figure 2. (+) ESI 9.4 T FT-ICR mass scale-expanded segment from m/z 542−547 for an oil spill contaminant at 2.5% percent formic acid concentration and analyte concentration 1.0 (top), 0.5 (middle), and 0.1 mg/mL (bottom). Elemental compositions are assigned only for peaks with magnitude greater than 6σ of rms baseline noise.

DOI: 10.1021/acs.energyfuels.7b03204
Energy Fuels 2018, 32, 2901−2907

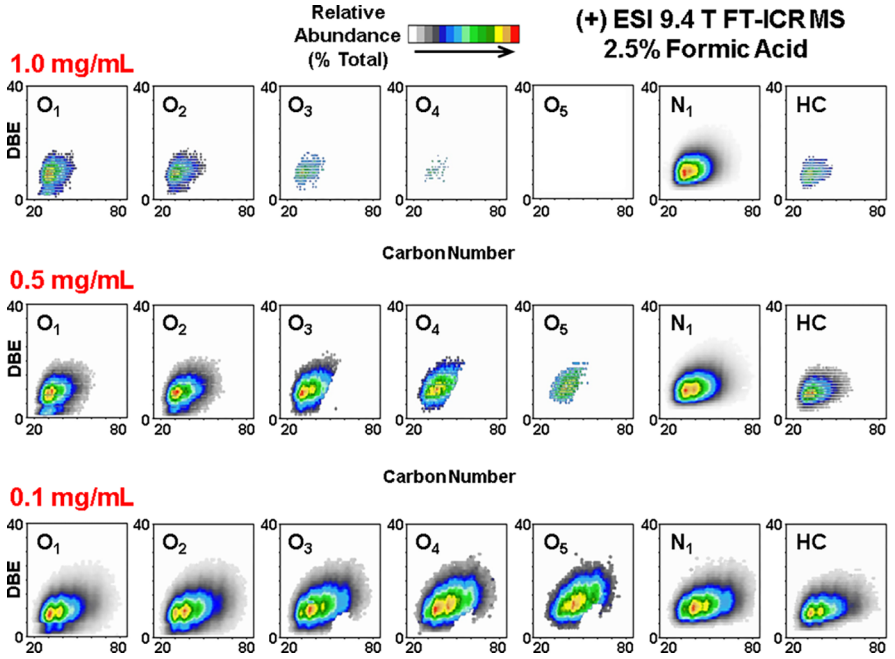

Figure 3. O_1, O_2, O_3, O_4, O_5, N_1, and HC heteroatom class isoabundance-contoured DBE vs carbon number plots for an oil spill contaminant at 2.5% percent formic acid concentration and analyte concentration 1.0 (top), 0.5 (middle), and 0.1 mg/mL (bottom).

abundance distributions in Figure 1 and detection of the suppressed ions at a given nominal mass shown in Figure 2.

The dramatic improvement in detection sensitivity for O_x species is evident from the plots of isoabundance-contoured DBE vs carbon number for O_{1-5}, N_1, and HC heteroatom classes presented in Figure 3. Hydrocarbon class compounds have not previously been detected by electrospray ionization, except as Ag^+ cation adducts[51] or by negative ESI in the presence of tetramethylammonium hydroxide as a strong base modifier[23] (present mechanism is unknown). At 1 mg/mL analyte concentration, O_4 and O_5 classes are below the detection threshold, and members of the N_1 class cluster narrowly near DBE ≈ 10 and carbon number ~25. At lower analyte concentration (0.1 mg/mL, bottom), the aforementioned O_5 class (undetected at 1.0 mg/mL) spans a wide range centered at DBE ≈ 12 and carbon number ~42, and the N_1 class extends to higher DBE and much higher carbon number. At 0.1 mg/mL analyte concentration, all heteroatom classes detected at greater than 1% relative abundance exhibit a wider compositional range at 0.1 mg/mL than at 1.0 mg/mL analyte concentration. Apparent loss in detection in the 0.1 mg/mL concentration O_3–O_5 class is actually loss of instrumental resolving power needed to resolve the systematic 1.7 mDa split between $C_2N_1{}^{13}C_1$ and H_3O_3 species (Supporting Information, Figures S1 and S2). That split requires an instrumental resolving power from 58 800 at m/z 100 to 588 000 at m/z 1000. The instrument used in this study begins to lose the required resolving power to resolve these particular splits at m/z 700 and higher.

Figure 4 shows positive ion electrospray FT-ICR MS heteroatom class distributions for the 0.1 mg/mL oil spill contaminant at various concentrations of formic acid. For a given analyte concentration, higher acid concentration in the spray mixture results in higher relative abundance of oxygen (O_{1-6}) relative to nitrogen (N_1) classes. Figure 5 shows results for a crude oil sample that is less oxygenated than the oil spill contaminant (by a factor of 5, measured by bulk elemental composition, data not shown). The dominant oxygen class is S_1O_1 and its relative

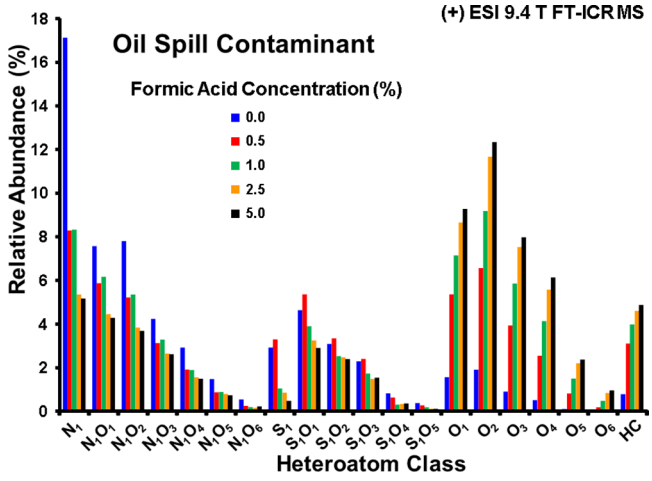

Figure 4. Heteroatom class distribution for a (+) ESI oil spill contaminant at analyte concentration 0.1 mg/mL and formic acid concentration of 0.0% (blue), 0.5% (red), 1.0% (green), 2.5% (orange), and 5.0% (black).

abundance and compositional range increase dramatically at lower analyte concentration and fixed formic acid concentration. We note the decreased S_1O_1% relative abundance in Figure 4 and increased S_1O_1% relative abundance in Figure 5. However, the S_1O_1 molecular elemental compositions in Figures 4 and 5 may not correspond to the same functional group. Moreover, compositional coverage and location in carbon number and DBE space improve for all heteroatom classes in the 0.1 mg/mL spectra, so that S_1O_1 relative abundance could decrease, even if the absolute number of such species increases.

Model Compound Analysis. An equimolar model compound mixture (six compounds) was prepared and serially diluted. TOF mass spectra for four of the eight dilutions are shown in Figure 6. As for the broadband FT-ICR mass spectra in the previous figures, at high analyte concentration (10 mM, top) pyridinic nitrogen compounds (m/z 158 and 258) and to

DOI: 10.1021/acs.energyfuels.7b03204
Energy Fuels 2018, 32, 2901−2907

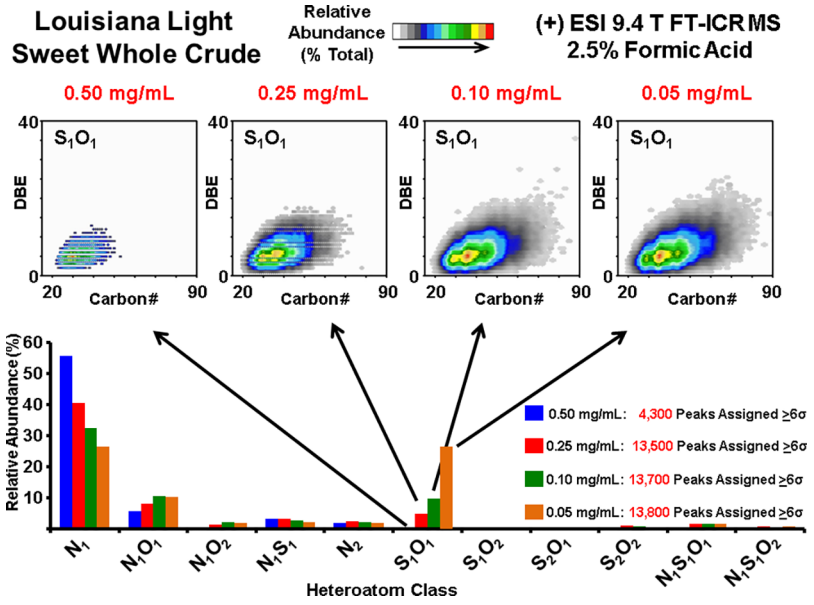

Figure 5. Heteroatom class distribution and corresponding S_1O_1 heteroatom class isoabundance-contoured DBE vs carbon number plots for crude oil at 2.5% formic acid concentration and analyte concentration 0.5 (blue), 0.25 (red), 0.10 (green), and 0.05 mg/mL (magenta).

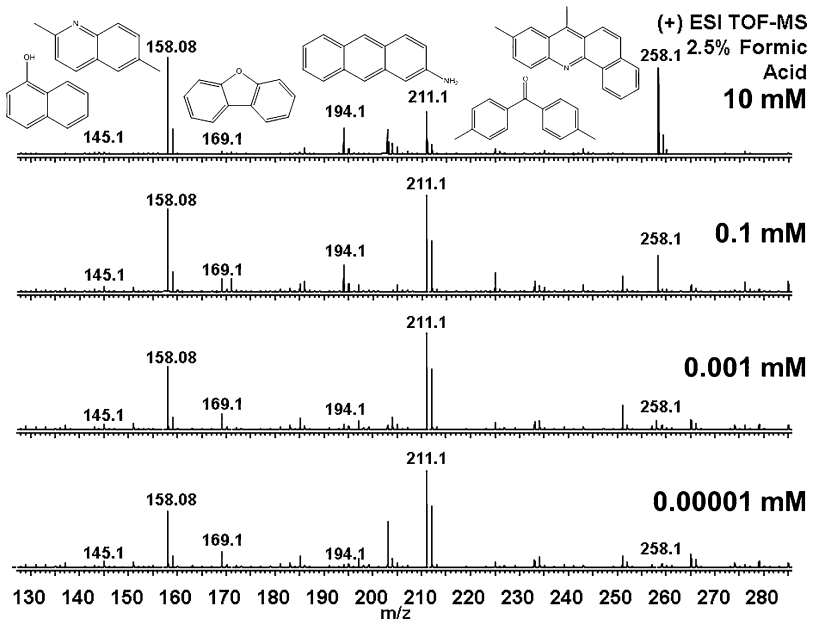

Figure 6. (+) TOF mass spectra (2.5% formic acid concentration) for an equimolar model compound mixture (proceeding from top to bottom): 10, 10^{-1}, 10^{-3}, and 10^{-5} mM. From left to right, the compounds are 1-naphthol (m/z 145.1), 2,6-dimethylquinoline (m/z 158.1), dibenzofuran (m/z 169.1), 2-aminoanthracene (m/z 194.1), 4,4′-dimethylbenzophenone (m/z 211.1), and 7,9 dimethylbenzacridine (m/z 258.1).

a lesser extent the amine compound (m/z 194) are preferentially ionized relative to the oxygen compounds (phenol, furan, and ketone; m/z 145, 169, and 211). As the concentration of the model compound mixture is reduced at constant formic acid concentration (2.5% v:v, which was chosen due to preferential spray stability over 5.0% v:v formic acid), the ionization efficiencies for all of the oxygen-containing compounds (especially the ketone) increase relative to those for the nitrogen-containing compounds (see Figure 7). Additional unassigned peaks are from crude oil carryover. Figure 7 shows the TOF signal intensity ratio for all oxygen-containing ions relative to all nitrogen-containing ions as a function of $\log_{10}$[total mixture concentration]. As the concentration of the equimolar mixture is reduced, the O/N signal intensity ratio increases asymptotically to a maximum. Increased ionization efficiency for oxygen-containing compounds is preserved in the presence of a proportionately concentrated oil spill contaminant mixture, as shown in Figure 8. One might expect that the ratio of oxygen to nitrogen should reach 1.2 (as in Figure 7); however, the FT-ICR lower mass limit precludes detection of species of m/z < 200, particularly 2,6-dimethylquinoline (m/z 158).

From the various results described above, it is clear that, at high analyte/formic acid concentration ratio, positive-ion ESI mass spectra are dominated by the most basic analytes (e.g., compounds containing pyridinic nitrogen).[26,52] Electrospray ionization begins from small droplets, each of which can accommodate only a limited number of charges.[31,53,54] Thus, at high analyte concentration, most of the droplet charge will reside on the

DOI: 10.1021/acs.energyfuels.7b03204
Energy Fuels 2018, 32, 2901−2907

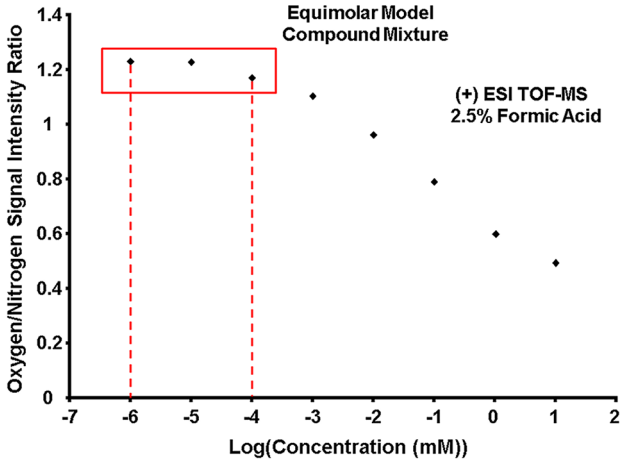

Figure 7. TOF mass spectral signal intensity ratio of all oxygen-containing to all nitrogen-containing ions versus log[concentration (mM)] of the equimolar model compound mixture shown in Figure 6.

most basic components. At sufficiently low analyte concentration, there are not enough basic molecules to accept the charge that can be accommodated in a droplet, and other (less basic) protonated molecules can accept the rest. These results are consistent with literature findings. Acetic acid, a somewhat weaker acid than formic, is also a popular choice for acid modifier in positive mode electrospray, and although it was not tested in this study, we believe it may have a similar effect in providing ionization coverage at high concentration.

The same argument should apply to the most acidic components for negative electrospray ionization; however, we did not observe changes in relative abundance of species of various acidity as a function of analyte/NH_4OH concentration for the samples in this study (data not shown), perhaps because NH_4OH is a weak base, so that only the strongest acids (carboxylic) deprotonate. Recently a stronger base modifier $(CH_3)_4NOH$ has been shown to dramatically increase ionization of weaker acids.[23] In any case, the present method does significantly enhance the compositional coverage for positive electrospray ionization.

CONCLUSION

Here, we demonstrate ionization bias in positive ion electrospray complex mixture analysis that can be quite severe for oxygenated petroleum complex mixtures. A 3-fold loss in number of detected species can occur over 1 order of magnitude concentration range at given acid modifier concentration, resulting in failure to detect as many as tens of thousands of molecular elemental compositions. We reproduce the petroleum heteroatom behavior with the model compound study to illustrate the competition between single heteroatom nitrogen and single heteroatom oxygen. We conclude that the behavior is strongly influenced by the competition for protons by pyridinic nitrogen and carbonyl oxygen.

ASSOCIATED CONTENT

Supporting Information

The Supporting Information is available free of charge on the ACS Publications website at DOI: 10.1021/acs.energyfuels.7b03204.

Figure S1: Figure 3 with red rings added to denote regions of unresolved 1.7 mDa splits between $C_2N_1{}^{13}C_1$ and H_3O_3. (PDF)

Figure S2: 1.7 mDa mass splits differing in elemental composition by $C_2N_1{}^{13}C_1$ vs H_3O_3. (PDF)

AUTHOR INFORMATION

Corresponding Author

*Phone: +1 850-644-0711. Fax: +1 850-644-1366. E-mail: hendrick@magnet.fsu.edu (C.L.H.).

*Phone: +1 850-644-2398. Fax: +1 850-644-1366. E-mail: rodgers@magnet.fsu.edu (R.P.R.).

*Phone: +1 850-644-0529. Fax: +1 850-644-0133. E-mail: marshall@magnet.fsu.edu (A.G.M.).

ORCID

Brian M. Ruddy: 0000-0001-5027-6804

Ryan P. Rodgers: 0000-0003-1302-2850

Alan G. Marshall: 0000-0001-9375-2532

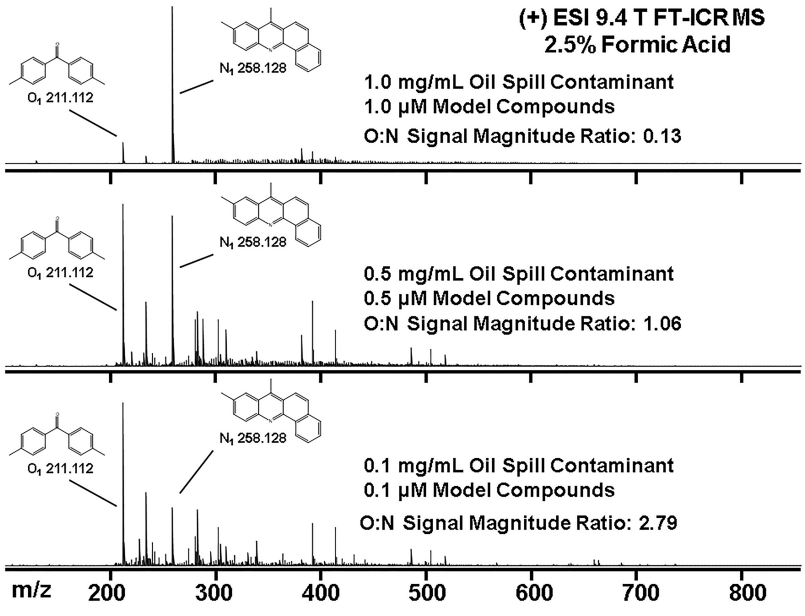

Figure 8. Broadband positive ion electrosprayed 9.4 T FT-ICR model compound mixture (1.0 (top), 0.5 (middle), and 0.1 μM (bottom)) spiked into a proportionately concentrated oil spill contaminant solution at 2.5% formic acid concentration.

DOI: 10.1021/acs.energyfuels.7b03204
Energy Fuels 2018, 32, 2901−2907

Notes

The authors declare no competing financial interest.

■ ACKNOWLEDGMENTS

This work was supported by the National Science Foundation Division of Materials Research through DMR-11-57490, CHE-10-49753 (RAPID). The Gulf of Mexico Research Initiative to the Deep-C Consortium, and the State of Florida. Special thanks go to John Quinn for continued assistance in instrument design, construction, and maintenance.

■ REFERENCES

(1) Hsu, C. S.; Liang, Z.; Campana, J. E. Hydrocarbon Characterization by Ultrahigh Resolution Fourier Transform Ion Cyclotron Resonance Mass Spectrometry. *Anal. Chem.* **1994**, *66*, 850−855.

(2) Marshall, A. G.; Rodgers, R. P. Petroleomics: The next grand challenge for chemical analysis. *Acc. Chem. Res.* **2004**, *37*, 53−59.

(3) Rodgers, R. P.; Schaub, T. M.; Marshall, A. G. Petroleomics: MS returns to its roots. *Anal. Chem.* **2005**, *77* (1), 20A−27A.

(4) Rodgers, R. P.; McKenna, A. M. Petroleum Analysis. *Anal. Chem.* **2011**, *83* (12), 4665−4687.

(5) Zhan, D.; Fenn, J. B. Electrospray mass spectrometry of fossil fuels. *Int. J. Mass Spectrom.* **2000**, *194*, 197−208.

(6) Lu, J.; Zhang, Y.; Shi, Q. Ionizing Aromatic Compounds in Petroleum by Electrospray with HCOONH4 as Ionization Promoter. *Anal. Chem.* **2016**, *88* (7), 3471−3475.

(7) Chen, R.; Yalcin, T.; Wallace, W. E.; Guttman, C. M.; Li, L. Laser desorption ionization and MALDI time-of-flight mass spectrometry for low molecular mass polyethylene analysis. *J. Am. Soc. Mass Spectrom.* **2001**, *12* (11), 1186−1192.

(8) Schaub, T. M.; Hendrickson, C. L.; Qian, K.; Quinn, J. P.; Marshall, A. G. High-Resolution Field Desorption/Ionization Fourier Transform Ion Cyclotron Resonance Mass Analysis of Nonpolar Molecules. *Anal. Chem.* **2003**, *75* (9), 2172−2176.

(9) Amirav, A.; Gordin, A.; Tzanani, N. Supersonic gas chromatography/mass spectrometry. *Rapid Commun. Mass Spectrom.* **2001**, *15* (10), 811−820.

(10) Gao, J.; Owen, B. C.; Borton, D. J.; Jin, Z.; Kenttamaa, H. I. HPLC/APCI Mass Spectrometry of Saturated and Unsaturated Hydrocarbons by Using Hydrocarbon Solvents as the APCI Reagent and HPLC Mobile Phase. *J. Am. Soc. Mass Spectrom.* **2012**, *23* (5), 816−822.

(11) Purcell, J. M.; Hendrickson, C. L.; Rodgers, R. P.; Marshall, A. G. Atmospheric Pressure Photoionization Fourier Transform Ion Cyclotron Resonance Mass Spectrometry for Complex Mixture Analysis. *Anal. Chem.* **2006**, *78* (16), 5906−5912.

(12) Corilo, Y. E.; Vaz, B. G.; Simas, R. C.; Nascimento, H. D. L.; Klitzke, C. F.; Pereira, R. C. L.; Bastos, W. L.; Neto, E. V. S.; Rodgers, R. P.; Eberlin, M. N. Petroleomics by EASI (±) FT-ICR MS. *Anal. Chem.* **2010**, *82*, 3990−3996.

(13) Wu, C.; Qian, K.; Nefliu, M.; Cooks, R. G. Ambient analysis of saturated hydrocarbons using discharged-induced oxidation in desorption electrospray ionization. *J. Am. Soc. Mass Spectrom.* **2010**, *21* (2), 261−267.

(14) Eckert, P. A.; Roach, P. J.; Laskin, A.; Laskin, J. Chemical Characterization of Crude Petroleum Using Nanospray Desorption Electrospray Ionization Coupled with High-Resolution Mass Spectrometry. *Anal. Chem.* **2012**, *84* (3), 1517−1525.

(15) Pérez, J.; Ramírez-Arizmendi, L. E.; Petzold, C. J.; Guler, L. P.; Nelson, E. D.; Kenttämaa, H. I. Laser-induced acoustic desorption/chemical ionization in Fourier-transform ion cyclotron resonance mass spectrometry. *Int. J. Mass Spectrom.* **2000**, *198* (3), 173−188.

(16) Nyadong, L.; McKenna, A. M.; Hendrickson, C. L.; Rodgers, R. P.; Marshall, A. G. Atmospheric Pressure Laser-Induced Acoustic Desorption Chemical Ionization Fourier Transform Ion Cyclotron Resonance Mass Spectrometry for the Analysis of Complex Mixtures. *Anal. Chem.* **2011**, *83* (5), 1616.

(17) Pomerantz, A. E.; Hammond, M. R.; Morrow, A. L.; Mullins, O. C.; Zare, R. N. Two-Step Laser Mass Spectrometry of Asphaltenes. *J. Am. Chem. Soc.* **2008**, *130* (23), 7216−7217.

(18) Rummel, J. L.; McKenna, A. M.; Marshall, A. G.; Eyler, J. R.; Powell, D. H. The coupling of direct analysis in real time ionization to Fourier transform ion cyclotron resonance mass spectrometry for ultrahigh-resolution mass analysis. *Rapid Commun. Mass Spectrom.* **2010**, *24* (6), 784−790.

(19) Smith, D. F.; McKenna, A. M.; Corilo, Y. E.; Rodgers, R. P.; Marshall, A. G.; Heeren, R. M. A. Direct Analysis of Thin-Layer Chromatography Separations of Petroleum Samples by Laser Desorption Ionization Fourier Transform Ion Cyclotron Resonance Mass Spectrometry Imaging. *Energy Fuels* **2014**, *28* (10), 6284−6288.

(20) Nyadong, L.; Inutan, E.; Wang, X.; Hendrickson, C. L.; Trimpin, S.; Marshall, A. G. Laserspray and Matrix-Assisted Ionization Inlet Coupled to High-Field Fourier Transform Ion Cyclotron Resonance Mass Spectrometry for Peptide and Protein Analysis. *J. Am. Soc. Mass Spectrom.* **2013**, *24* (3), 320−328.

(21) Dole, M.; Mack, L. L.; Hines, R. L.; Mobley, R. C.; Ferguson, L. D.; Alice, M. B. Molecular Beams of Macroions. *J. Chem. Phys.* **1968**, *49*, 2240.

(22) Yamashita, M.; Fenn, J. B. Electrospray ion source. Another variation of the free-jet theme. *J. Phys. Chem.* **1984**, *88* (20), 4451−4459.

(23) Lobodin, V. V.; Juyal, P.; McKenna, A. M.; Rodgers, R. P.; Marshall, A. G. Tetramethylammonium Hydroxide as a Reagent for Complex Mixture Analysis by Negative Ion Electrospray Ionization Mass Spectrometry. *Anal. Chem.* **2013**, *85* (16), 7803−7808.

(24) Qian, K.; Rodgers, R. P.; Hendrickson, C. L.; Emmett, M. R.; Marshall, A. G. Reading Chemical Fine Print: Resolution and Identification of 3000 Nitrogen-Containing Aromatic Compounds from a Single Electrospray Ionization Fourier Transform Ion Cyclotron Resonance Mass Spectrum of Heavy Petroleum Crude Oil. *Energy Fuels* **2001**, *15* (2), 492−498.

(25) Hughey, C. A.; Rodgers, R. P.; Marshall, A. G.; Qian, K.; Robbins, W. R. Identification of acidic NSO compounds in crude oils of different geochemical origins by negative ion electrospray Fourier Tansform Ion Cyclotron Resonance Mass Spectrometry. *Org. Geochem.* **2002**, *33*, 743−759.

(26) Qian, K.; Robbins, W. K.; Hughey, C. A.; Cooper, H. J.; Rodgers, R. P.; Marshall, A. G. Resolution and Identification of Elemental Compositions for More than 3000 Crude Acids in Heavy Petroleum by Negative-Ion Microelectrospray High-Field Fourier Transform Ion Cyclotron Resonance Mass Spectrometry. *Energy Fuels* **2001**, *15* (6), 1505−1511.

(27) King, R.; Bonfiglio, R.; Fernandez-Metzler, C.; Miller-Stein, C.; Olah, T. Mechanistic investigation of ionization suppression in electrospray ionization. *J. Am. Soc. Mass Spectrom.* **2000**, *11* (11), 942−950.

(28) Müller, C.; Schäfer, P.; Störtzel, M.; Vogt, S.; Weinmann, W. Ion suppression effects in liquid chromatography−electrospray-ionisation transport-region collision induced dissociation mass spectrometry with different serum extraction methods for systematic toxicological analysis with mass spectra libraries. *J. Chromatogr. B: Anal. Technol. Biomed. Life Sci.* **2002**, *773* (1), 47−52.

(29) Gustavsson, S. Å.; Samskog, J.; Markides, K. E.; Långström, B. Studies of signal suppression in liquid chromatography−electrospray ionization mass spectrometry using volatile ion-pairing reagents. *Journal of Chromatography A* **2001**, *937* (1), 41−47.

(30) Benijts, T.; Dams, R.; Lambert, W.; De Leenheer, A. Countering matrix effects in environmental liquid chromatography−electrospray ionization tandem mass spectrometry water analysis for endocrine disrupting chemicals. *Journal of Chromatography A* **2004**, *1029* (1), 153−159.

(31) Enke, C. G. A Predictive Model for Matrix and Analyte Effects in Electrospray Ionization of Singly-Charged Ionic Analytes. *Anal. Chem.* **1997**, *69* (23), 4885−4893.

(32) Kloepfer, A.; Quintana, J. B.; Reemtsma, T. Operational options to reduce matrix effects in liquid chromatography−electrospray

DOI: 10.1021/acs.energyfuels.7b03204
Energy Fuels 2018, 32, 2901−2907

ionisation-mass spectrometry analysis of aqueous environmental samples. *Journal of Chromatography A* **2005**, *1067* (1), 153−160.
(33) Schuhmacher, J.; Zimmer, D.; Tesche, F.; Pickard, V. Matrix effects during analysis of plasma samples by electrospray and atmospheric pressure chemical ionization mass spectrometry: practical approaches to their elimination. *Rapid Commun. Mass Spectrom.* **2003**, *17* (17), 1950−1957.
(34) Taylor, P. J. Matrix effects: the Achilles heel of quantitative high-performance liquid chromatography−electrospray−tandem mass spectrometry. *Clin. Biochem.* **2005**, *38* (4), 328−334.
(35) Page, J. S.; Marginean, I.; Baker, E. S.; Kelly, R. T.; Tang, K.; Smith, R. D. Biases in Ion Transmission Through an Electrospray Ionization-Mass Spectrometry Capillary Inlet. *J. Am. Soc. Mass Spectrom.* **2009**, *20* (12), 2265−2272.
(36) Shuford, C. M.; Muddiman, D. C. Capitalizing on the hydrophobic bias of electrospray ionization through chemical modification in mass spectrometry-based proteomics. *Expert Rev. Proteomics* **2011**, *8* (3), 317−323.
(37) Furey, A.; Moriarty, M.; Bane, V.; Kinsella, B.; Lehane, M. Ion suppression; A critical review on causes, evaluation, prevention and applications. *Talanta* **2013**, *115*, 104−122.
(38) Cheng, Z. L.; Siu, K. W. M.; Guevremont, R.; Berman, S. S. Electrospray mass spectrometry: a study on some aqueous solutions of metal salts. *J. Am. Soc. Mass Spectrom.* **1992**, *3* (4), 281−288.
(39) Frahm, J. L.; Muddiman, D. C.; Burke, M. J. Leveling Response Factors in the Electrospray Ionization Process Using a Heated Capillary Interface. *J. Am. Soc. Mass Spectrom.* **2005**, *16* (5), 772−778.
(40) Kaiser, N. K.; Quinn, J. P.; Blakney, G. T.; Hendrickson, C. L.; Marshall, A. G. A novel 9.4 T FTI-CR Mass Spectrometer with Improved Sensitivity, Mass Resolution and Mass Range. *J. Am. Soc. Mass Spectrom.* **2011**, *22*, 1343−1351.
(41) Blakney, G. T.; Hendrickson, C. L.; Marshall, A. G. Predator data station: A fast acquisition system for advanced FT-ICR MS experiments. *Int. J. Mass Spectrom.* **2011**, *306*, 246−252.
(42) Podgorski, D. C.; Mckenna, A. M.; Rodgers, R. P.; Marshall, A. G.; Cooper, W. T. Selective Ionization of Dissolved Organic Nitrogen by Positive Ion Atmospheric Pressure Photoionization Coupled with Fourier Transform Ion Cyclotron Resonance Mass Spectrometry. *Anal. Chem.* **2012**, *84*, 5085−5090.
(43) Xian, F.; Hendrickson, C. L.; Blakney, G. T.; Beu, S. C.; Marshall, A. G. Automated Broadband Phase Phase Correction of Fourier Transform Ion Cyclotron Resonance Mass Spectra. *Anal. Chem.* **2010**, *82*, 8807−8812.
(44) Comisarow, M. B.; Marshall, A. G. Selective-phase Ion Cyclotron Resonance Spectroscopy. *Can. J. Chem.* **1974**, *52*, 1997−1999.
(45) Marshall, A. G.; Comisarow, M. B.; Parisod, G. Relaxation and spectral line shape in Fourier transform ion resonance spectroscopy. *J. Chem. Phys.* **1979**, *71* (11), 4434−4444.
(46) Beu, S. C.; Blakney, G. T.; Quinn, J. P.; Hendrickson, C. L.; Marshall, A. G. Broadband phase correction of FT-ICR mass spectra via simultaneous excitation and detection. *Anal. Chem.* **2004**, *76* (19), 5756−5761.
(47) Xian, F.; Corilo, Y. E.; Hendrickson, C. L.; Marshall, A. G. Baseline correction of absorption-mode Fourier transform ion cyclotron resonance mass spectra. *Int. J. Mass Spectrom.* **2012**, *325−327* (0), 67−72.
(48) Savory, J. J.; Kaiser, N. K.; McKenna, A. M.; Xian, F.; Blakney, G. T.; Rodgers, R. P.; Hendrickson, C. L.; Marshall, A. G. Parts-Per-Billion Fourier Transform Ion Cyclotron Resonance Mass Measurement Accuracy with a 'Walking' Calibration Equation. *Anal. Chem.* **2011**, *83*, 1732−1736.
(49) Hughey, C. A.; Hendrickson, C. L.; Rodgers, R. P.; Marshall, A. G.; Qian, K. Kendrick Mass Defect Spectrum: A Compact Visual Analysis for Ultrahigh-Resolution Broadband Mass Spectra. *Anal. Chem.* **2001**, *73* (19), 4676−4681.
(50) McLafferty, F. W.; Turecek, F. *Interpretation of Mass Spectra*, 4th ed.; University Science Books: Mill Valley, CA, 1993.
(51) Lobodin, V. V.; Juyal, P.; McKenna, A. M.; Rodgers, R. P.; Marshall, A. G. Silver Cationization for Rapid Speciation of Sulfur-Containing Species in Crude Oils by Positive Electrospray Ionization Fourier Transform Ion Cyclotron Resonance Mass Spectrometry. *Energy Fuels* **2014**, *28* (1), 447−452.
(52) Hughey, C. A.; Rodgers, R. P.; Marshall, A. G. Resolution of 11000 Compositionally Distinct Components in a Single Electrospray Ionization Fourier Transform Ion Cyclotron Resonance Mass Spectrum of Crude Oil. *Anal. Chem.* **2002**, *74* (16), 4145−4149.
(53) Cech, N. B.; Enke, C. G. Effect of Affinity for Droplet Surfaces on the Fraction of Analyte Molecules Charged during Electrospray Droplet Fission. *Anal. Chem.* **2001**, *73* (19), 4632−4639.
(54) Mora, J. F. d. l.; Van Berkel, G. J.; Enke, C. G.; Cole, R. B.; Martinez-Sanchez, M.; Fenn, J. B. Electrochemical processes in electrospray ionization mass spectrometry. *J. Mass Spectrom.* **2000**, *35* (8), 939−952.

DOI: 10.1021/acs.energyfuels.7b03204
Energy Fuels 2018, 32, 2901−2907